PREDICTING INTERNAL YELLOW-POPLAR LOG DEFECT FEATURES USING SURFACE INDICATORS

*R. Edward Thomas**

USDA Forest Service
Northern Researh Station
Princeton, WV 24740

(Received July 2007)

ABSTRACT

Determining the defects that are located within the log is crucial to understanding the tree/log resource for efficient processing. However, existing means of doing this non-destructively requires the use of expensive X-ray/CT, MRI, or microwave technology. These methods do not lend themselves to fast, efficient, and cost-effective analysis of logs and tree stems in the mill. This study quantified the relationship between external defect indicators and internal defect characteristics for yellow-poplar logs. A series of models were developed to predict internal features using visible external features, log diameter, indicator width, length, and rise. Good correlations and small prediction errors were observed with sound (sawn), overgrown, and unsound knot defects. For less severe defects such as adventitious buds/clusters and distortion type defects weaker correlations were observed, but the magnitude of prediction errors was small and acceptable.

Keywords. Yellow-poplar, hardwood log, defect modeling, internal defect prediction, external indicator.

INTRODUCTION

One of the major emphasis areas today in hardwood research is the development of equipment and a methodology that can accurately sense internal defect locations and structures. Determining the location and characteristics of defects located inside logs promises to dramatically improve log recovery in terms of both quantity and quality (Steele et al. 1994). In addition, accurate internal defect information would permit researchers to analyze, refine, and expand log grading rules, multi-product potential, stand differences, and the impact of silvicultural treatments on quality in ways previously not available or economically feasible. The goal of this research is to provide a mathematical method of predicting internal defect size and location based on external surface indicators. This study was limited to the most common defect types that are those that have the greatest impact on hardwood quality (tree or lumber grade).

Although there are many benefits to determining internal log information, an inexpensive and efficient method of obtaining these data does not exist today. Researchers are currently examining various approaches to this problem including the use of X-ray/CT (computerized tomography), ultrasound, MRI (Magnetic Resonance Imaging), or radar technology (Chang 1992). Some high-volume softwood lumber mills in Europe and the Pacific Northwest have installed multiple-head X-ray scanners. This type of scanner uses 3 or 4 X-ray transmitters and detectors to capture internal log defect data. Although these types of scanners operate much faster, they obtain lower quality/resolution data than do CT scanners. Although X-ray/CT and MRI methods show promise, the technology is expensive, slow, and does not permit fast, efficient analysis of logs and tree stems. Both CT and three-head X-ray systems are still limited to being used on smaller-diameter logs due to energy level issues.

During the past 50 yr there has been a significant amount of research conducted examining the relationship of external hardwood log defect indicators to internal defect characteristics. Several guides and pictorial series have been pub-

* Corresponding author: ethomas@fs.fed.us

lished illustrating various external/internal defect characteristics and their relationship for various hardwood species (Marden and Stayton 1970; Rast 1982; Rast et al. 1985, 1988, 1989, 1990a, 1990b, 1990c). While these guides are useful references for providing insight on the external/internal relationship, only one or two examples of each defect type are provided. Thus, they do not fulfill the need of a definitive model capable of predicting internal defect features based on observable external defect features.

Researchers have studied the relationships among surface indicators and internal defect manifestation in depth for various hardwood and softwood species. Schultz (1961) examined German beech and found that for this species the ratio of the bark distortion width to length is the same as the ratio of the stem when the branch is completely healed over to the current stem diameter. However, for species with heavier irregular bark, like hard maple, he found that it was difficult to judge the clear area above the defect in this manner.

Hyvärinen (1976) used Stayton et al. (1970) maple defect data to explore the relationships among the internal features of grain orientation and height of clear wood above an encapsulated knot defect and the external features of surface rise, width, and length. The sugar maple defect data were collected from 44 trees obtained from three sites in upper Michigan. Hyvärinen used simple linear regression methods to find good correlations among clear wood above defects, bark distortion width, length, and rise measurements, as well as age, tree diameter, and stem taper. The best simple correlation was with diameter inside bark (DIB) ($r = 0.66$) and an 18-mm standard error of estimate. Correlation was further improved by using a stepwise regression method. The final model ($r = 0.74$) employed bark distortion vertical size and DIB as the most significant predictor variables.

A similar study was conducted on a sample of 21 black spruce trees collected from a natural stand 75 km north of Quebec City (Lemieux et al. 2001). Three trees, each with three logs, were selected from which a total of 249 knot defects were dissected and their data recorded. The researchers found better correlations between external indicator and internal characteristics in the middle and bottom logs as compared to the upper logs. Strong correlations ($r > .89$) among the length and width of internal defect zones and external features such as branch stub diameter and length were found to exist. The defects were modeled as having three distinct zones corresponding to the manner in which the penetration angle changes over time in black spruce. The penetration angle is the angle at which a line through the center of the defect intersects the log surface. This study examined only branches that had not been dropped nor pruned and thus could not examine encapsulation depth.

Carpenter (1950) found that although the frequency and occurrence of surface indicators within a given species vary by region, in general the same indicator will be found with its defect in the underlying wood. Thus, although certain defect types may be more prevalent in some regions, the underlying manifestation of the defect would remain more or less consistent across regions. Further, growth rate will vary from region to region (or site to site within the same region), thus the defect encapsulation rate will differ also. However, the rate at which the encapsulation occurs, and the degree to which the defect is occluded or covered over by clear wood is indicated in the bark pattern. Shigo and Larson (1969) discovered that the ratio of defect height-to-width indicates the depth of the defect with respect to the radius of the stem at the defect (Fig. 1). The faster the diameter growth, the faster the defect is encapsulated, and thus the faster the bark distortion pattern changes.

MATERIALS AND METHODS

Sample collection

Yellow-poplar defect samples were collected from two sites in West Virginia: West Virginia University Forest (WVUF) near Morgantown (elevation: 700 m) and Camp Creek State Forest (CCSF) near Princeton (elevation: 790 m). The two sites are separated by approximately 350 km. From each site, 33 trees were randomly se-

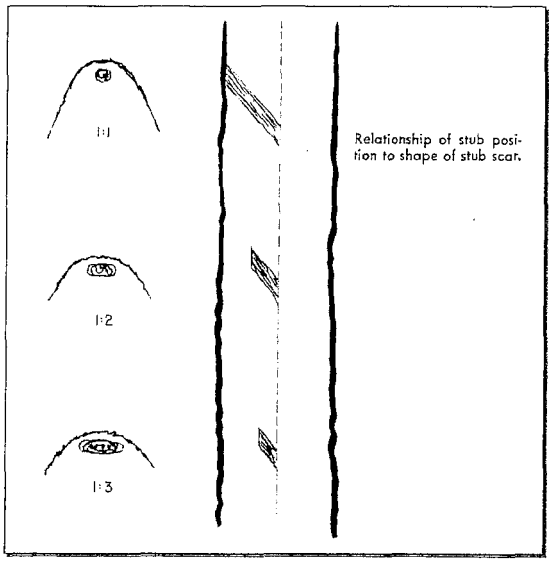

FIG. 1. Encapsulation depth and stub scar relationship ratio.

lected. For each tree, the number of defects by type were counted. The types of defects identified, counted, and analyzed in this study are listed in Table 1. These counts were used to develop a random sampling plan. The goal was to collect 4 defects of each type from each tree, whenever possible. For example, if there were 8 sound knots on the tree, every second sound knot was selected. Of course, not all trees had 4 defects of every type. In other cases, selecting one defect would prevent another from being selected due to defect overlap. Defects are overlapping when the process of bucking the defect from the log and processing it would destroy all or part of another. In these cases, preference went to the defect type that was more numerous on that tree and a different occurrence of the other defect selected.

TABLE 1. *Types and numbers of defects collected by site and overall.*

Defect name	Defect abbreviation	Location		Total
		CCSF	WVU forest	
Adventitious knot	AK	75	66	141
Adventitious knot cluster	AKC	59	68	127
Bump	BUMP	3	1	4
Heavy distortion	HD	74	60	134
Light distortion	LD	98	6	104
Medium distortion	MD	91	79	170
Overgrown knot	OK	87	76	163
Overgrown knot cluster	OKC	20	1	21
Sound knot	SK	41	31	72
Sound knot cluster	SKC	2	0	2
Unsound knot	UK	6	33	39
Wound	WND	14	13	27
Total		570	434	1004

The number of defect samples obtained from each site by defect type is shown in Table 1. In most cases, approximately equal numbers of each type of defect were obtained from each site. The exceptions are the light distortion (LD) and unsound knot (UK) defects. UK defects occurred in much fewer numbers at CCSF than at WVUF. More LD defects were found on CCSF samples than the ones from WVUF.

Sample processing

All defects were identified according to the characteristics as defined in *Defects in Hardwood Timber* (Carpenter et al. 1989). Once a defect was located and classified, the section containing the defect was cut from the log. The defect sections ranged from 305 to 310 mm in length. If we discovered during slicing that part of the interior defect was not completely contained within the section, the sample was discarded. An alignment groove was cut into the top of the section in a line between the indicator and the pith. This provided a smooth area for easier ring counts and a common point of reference for each slice for collection position/offset measurements. An identifying tag was stapled to the section surface and the defect indicator was digitally photographed (Fig. 2). The tag identifies the source tree and log, defect type, defect number, and height up the stem.

For each sample the following information was recorded: defect type, surface width (across grain) and length (along grain), growth rate, bark thickness, and surface height rise, if any. The sample was then sawn into 25-mm-thick slices at 90° to the reference notch. This resulted in a series showing the defect penetrating the log

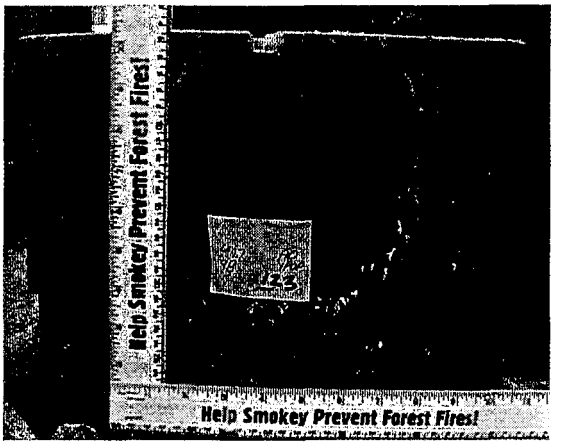

FIG. 2. Defect section with tagged defect and reference groove.

(Fig. 3). For each slice the depth, defect width, length, and distance of defect center to notch-bottom center were recorded. When a defect terminated between slices, it was assumed that it terminated at the halfway point through the slice.

Modeling statistics

A series of chi-squared tests were used to test for outliers in the internal/external data set (Komsta 2006). Data identified by the tests as outliers were examined and corrected if in error. The data were grouped by defect type. Using the statistics program "R," stepwise muliple-linear regression analyses were used to test for correlations among surface indicators and internal features (R Development Core Team 2006). The independent variables used were surface indicator width (SWID), length (SLEN), rise (SRISE), and log diameter inside bark (DIB). These variables were selected because they are measurable during log surface inspection. Area (SWID * SLEN), $SLEN^2$, $SWID^2$, and $SRISE^2$) and all other possible combinations of interaction terms were also examined as potential predictor variables. The dependent variables selected were 1) rake (penetration angle), 2) clear wood above defect, 3) total depth, 4) halfway-point cross-section width (HWID), and 5) halfway-point cross-section length (HLEN). These variables permit an internal model of a defect to be constructed and determine an approximate internal location (Fig. 4).

Within each defect type class, the data were randomly partitioned into two groups using the caTools package (Tuszynski 2006) for the R statistical analysis program. The first group contained 66.7% of the records and was used for model development and determining the internal/external feature correlation statistic. The second set contained the remaining records and was used for testing the prediction models (model validation set). Table 2 shows the numbers of observations used in the model development and testing steps. Adjusted multiple R^2 tests were

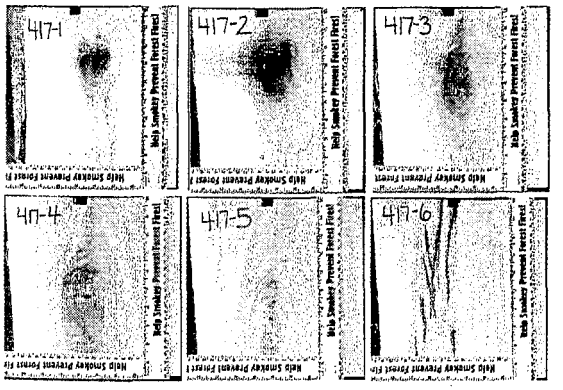

FIG. 3. Series of internal defect sections for surface indicator shown in Fig. 2.

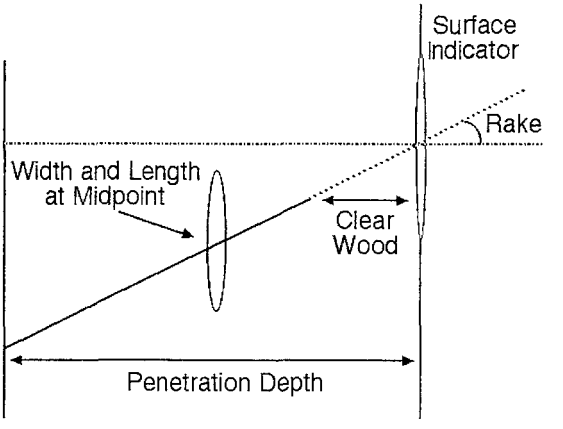

FIG. 4. Illustration of internal features predicted by the model.

TABLE 2. *Numbers of observations used in model development and testing by defect type.*

Defect code	Number of observations: Model dataset	Testing dataset	Total observations
AK	94	47	141
AKC	84	43	127
HD	89	45	134
LD	62	32	94
MD	113	57	170
OK	108	55	163
OKC	14	7	21
SK	48	24	72
UK	26	13	39

used to determine the correlation among external defect measurements and internal features. Adjusted R^2 is a modification of R^2 that adjusts for the number of explanatory terms in a model. Unlike R^2, the adjusted R^2 increases only if the new term improves the model more than would be expected by chance.

RESULTS AND DISCUSSION

Correlation results for model development and significant predictor variables are presented in Table 3. The number of overgrown knot cluster (OKC) defects was not sufficient for establishing a defect prediction model. Due to feature similarities between overgrown knots (OK) and overgrown knot clusters (OKC), data from these defect types were combined. This data set was then analyzed to see if the combined data could be used to predict internal features for OKC defects. A separate analysis was performed for overgrown knot model development and testing using only overgrown knot data. In addition, there was not a sufficient sample size of wound and bump defects for model development. These defect types have been excluded from further discussion here.

Knots and severe defects

In most instances, strong correlations were found to exist among external defect indicators and internal characteristics for severe defect types: OK, OKC, sound knots (SK), and unsound knots (UK). The strength of the relationship (adjusted multiple R^2) between the interior halfway point width (HWID) measurement and external features ranged from 0.47 to 0.73. Similar results were found to exist among external features and the halfway point length (HLEN) measurement (adjusted multiple R^2 from 0.46 to 0.73). Most of the severe defect observations terminated at the pith, approximately the center of the slab for most samples. This is demonstrated in the strong relationship among penetration depth and external features–specifically diameter with adjusted multiple R^2 ranging from 0.63 to 0.76. The strongest correlation for rake angle was for the sound knot defects (adjusted multiple $R^2 = 0.70$). However, in most cases, the relationship between rake and external features was not very strong with adjusted multiple R^2 ranging from 0.22 to 0.36 for the other severe knot defects. For all knot defects the correlations between external indicators and internal features were significant ($p < 0.01$). Clear area above an encapsulated defect is not normally present with knot defects; thus no model was pursued for this feature.

Table 3 lists the most significant independent or predictor variables for each defect type and internal feature. The independent variables are listed in the order of most to least significant. Correlations with diameter inside bark (DIB) and/or surface indicator length (SLEN) were the most common. DIB was a significant variable in 3 more instances (27 vs. 24) than SLEN, and DIB had a stronger influence in almost all cases. SRISE and SWID had significant influences on the external internal relations in fewer instances; 15 and 12, respectively. Interaction terms such as surface area (SWID*SLEN), volume (SWID*SLEN*SRISE), and others had a significant correlation to internal features in 11 instances.

The mean-absolute error (MAE) is the mean of the absolute value of the residual errors for the fitted equation. MAE indicates the +/– error range that can be expected using the fitted equation to predict defect features. The associated MAE with the model development samples were

TABLE 3. *Model development and testing correlation results.*

		Model development results				Model testing results		
Defect type	Dependent variable	Multiple adjusted R squared	Mean absolute error	Correlation significant?	Significant independent variables	Correlation coefficient 'R'	Mean absolute error	Correlation significant?
AK	Hwid	0.29	3.6	Yes	DIB, Srise SWid, SWid*SLen, SWid*SRise, SWid*DIB,	0.53	4.8	Yes
	Hlen	0.48	3.6	Yes	SWid*SLen*SRise	0.44	6.4	Yes
	Rake	0.20	4.09	Yes	SLen, SRise, SWid*SRise	0.11	6.65	No
	Depth	0.49	18.0	Yes	DIB, SRise	0.74	26.7	Yes
	Clear	0.07	20.1	No	DIB, SRise	0.33	21.1	Yes
AKC	Hwid	0.27	6.6	Yes	DIB, SWid, DIB*SWid	0.29	30.5	No
	Hlen	0.39	5.8	Yes	Swid, SWid*SLen	0.56	6.6	Yes
	Rake	—	—	No	SWid, Slen	—	—	No
	Depth	0.32	15.2	Yes	DIB, SWid, DIB*SWid	0.74	26.9	Yes
	Clear	0.15	16.3	Yes	SLen, SWid, SRise, SWid*SLen, SRise*SLen	0.17	20.6	No
HD	Hwid	0.36	5.3	Yes	DIB, SLen, DIB*SLen	0.63	17.5	Yes
	Hlen	0.34	8.6	Yes	DIB, SLen, DIB*SLen	0.67	10.2	Yes
	Rake	0.08	8.61	No	DIB, SRise	0.25	8.85	No
	Depth	0.76	11.4	Yes	DIB, SRise	0.90	11.2	Yes
	Clear	0.10	15.7	Yes	DIB, SRise	0.38	14.7	Yes
LD	Hwid	0.03	5.3	No	SLen	0.59	9.1	Yes
	Hlen	0.02	7.4	No	SLen	0.60	4.8	Yes
	Rake	0.07	8.12	No	SWid, SLen	0.26	8.83	No
	Depth	0.56	9.7	Yes	DIB, SWid	0.77	11.7	Yes
	Clear	0.18	20.8	Yes	DIB, SWid, DIB*SWid	0.37	21.1	No
MD	Hwid	0.25	5.1	Yes	DIB, SLen	0.35	7.9	Yes
	Hlen	0.27	7.1	Yes	DIB, SLen	0.37	7.1	Yes
	Rake	—	—	No	—	—	—	No
	Depth	0.81	10.9	Yes	DIB, SWid, SLen	0.84	11.2	Yes
	Clear	0.25	18.8	Yes	DIB, SWid, SLen	0.52	20.3	Yes
OK	Hwid	0.55	6.1	Yes	SLen, SLen*SWid, SWid*DIB	0.63	22.4	Yes
	Hlen	0.49	10.2	Yes	SLen*DIB	0.64	13.7	Yes
	Rake	0.31	8.56	Yes	DIB, SLen	0.46	8.84	Yes
	Depth	0.76	10.4	Yes	DIB, SWid	0.85	11.4	Yes
	Clear	—	—	No	—	—	—	No
OK/OKC	Hwid	0.47	6.9	Yes	DIB, SLen, SRise	0.44	22.6	Yes
	Hlen	0.46	12.2	Yes	DIB, SLen	0.47	15.2	Yes
	Rake	0.22	11.13	Yes	SLen, SRise	0.52	10.47	Yes
	Depth	0.73	10.7	Yes	DIB, SWid	0.86	11.4	Yes
	Clear	—	—	No	—	—	—	No
SK	Hwid	0.73	7.9	Yes	DIB, SWid, SLen	0.87	16.8	Yes
	Hlen	0.73	14.5	Yes	DIB, SWid, SRise	0.79	20.8	Yes
	Rake	0.70	8.75	Yes	SLen, SRise	0.71	13.80	Yes
	Depth	0.63	10.4	Yes	DIB, SLen	0.78	14.2	Yes
	Clear	—	—	No	—	—	—	No
UK	Hwid	0.70	7.1	Yes	DIB, SLen	0.76	19.1	Yes
	Hlen	0.65	17.0	Yes	SWid, SLen	0.45	32.0	No
	Rake	0.36	8.50	Yes	Slen	0.43	9.71	No
	Depth	0.70	12.2	Yes	DIB, SLen	0.45	22.1	No
	Clear	—	—	No	—	—	—	No

small in most cases. The MAE values in Table 3 are reported in millimeters for all measurements except rake angle, which is in degrees. In 10 out of 12 cases for the knot defects, the MAE is 13 mm or less. In the remaining two cases the MAE values are 15 and 17 mm for the halfway-in length measurements for sound and unsound knots. The MAE values for rake angle varied between 8 and 11°.

The model testing samples were used to analyze the predictive capabilities. The regression equations generated with the model development samples were used to predict internal feature measurements. The correlation coefficient, r, the mean absolute error (MAE), and the significance level of the correlation were determined for each defect type and feature combination (Table 3). For most knot defect types (overgrown, overgrown/overgrown knot clusters, and sound knots), all correlations were significant ($p < 0.01$). For the unsound knot defects, only the correlation of halfway point cross-section width was significant with a MAE of 19 mm. The best results were with sound knots with correlation coefficients (R) ranging from 0.71 to 0.87. The correlation coefficients with predicted depth for the overgrown knots and knot clusters were 0.85 and 0.86. Total depth had the smallest MAE, ranging from 11 to 14 mm. The rake MAE ranged between 8 and 14°. For a 400-mm-diameter log with a defect terminating near the center, a 10° error would change the defect center position by 43 (10° under-estimate) to 54 mm (10° over-estimate) at the pith, depending on angle (Fig. 5). The difference in defect position at the halfway point would have a maximum positional variance of 22 (10° under-estimate) to 27 mm (10° over-estimate) depending on degree.

Overall, with the exception of rake angle, the overgrown knot correlation results were better than those from the grouped overgrown knot and cluster data (Table 3). Further, the differences in predicted depth between the overgrown knot and cluster data were minimal. However, the differences between correlation results for predicted halfway-in width and length suggest that using a separate model for only overgrown knots is better than using the grouped knot and cluster model.

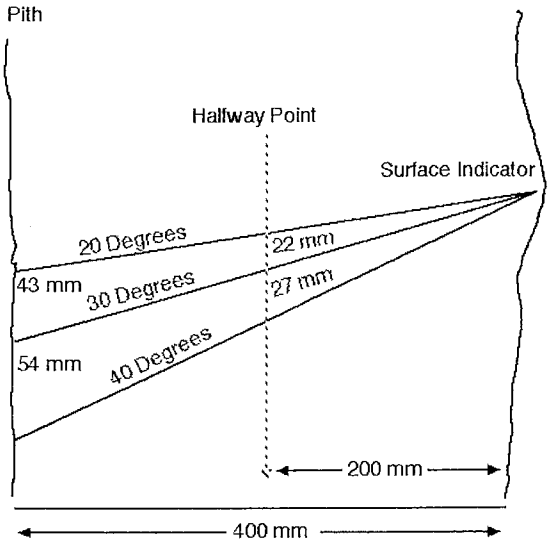

FIG. 5. Impact of rake error on internal defect position.

Bark distortions and adventitious defects

In general, the correlations between external indicator measurements and internal features for bark distortion and adventitious defects were not as strong as those measured for the severe knot defects. Distortion defects have been encapsulated longer than the more recent knot defects. Thus, less surface information is available for the distortion defect types. The model development correlation results are listed in Table 3.

The strongest correlations between external and internal features for the minor defects were with the adventitious defect types. Multiple adjusted R^2 for AK defects ranged from 0.20 to 0.48 for the correlations that were significant ($p < 0.01$). In addition, the MAE for the HWID and HLEN internal variables was 4 mm, in both cases. However, for AK defects the correlation between the clear area above the defect and external indicators was not significant ($p < 0.01$).

For AKC defects, all correlations among external indicators and internal features were significant ($p < 0.01$), with the exception of rake angle. Multiple adjusted R^2 for AKC defects

ranged from 0.15, for the clear area, to between 0.27 and 0.39 for the remaining internal features. The MAE for the internal features also was small with HWID and HLEN MAE values of 7 and 6 mm, respectively.

Good correlations between external and internal features were also found for the heavy and medium distortion defects. With the exception of rake, all correlations for these defects were significant ($p < 0.01$). The strongest relationship was associated with the prediction of total depth with adjusted R^2 values of 0.76 and 0.81 for heavy and medium distortions, respectively. The mean absolute errors for the fitted models were $\leq$5 mm for halfway-in width, <9 mm for halfway-in length, $\leq$11 mm for predicted depth, and 19 to 22 mm for encapsulation depth. For light distortion defects, depth was the only feature significantly related to external features with a multiple adjusted R^2 of 0.56 ($p < 0.01$).

All minor defect types had at least one feature that did not have a significant correlation with external features. Rake angle was the most difficult to predict internal feature with a significant correlation to external features found only with adventitious knots. In this case, the adjusted R^2 was low, but the mean absolute error was only 4.09°. The correlation among clear area above an encapsulated defect and external features was also weak with adjusted R^2 values ranging from 0.10 to 0.25.

Hyvarinen (1976) reported that the most common significant predictor variable for sugar maple clear area was DIB. Thus, these results are in agreement. Diameter was the most frequent significant predictor for the distortion and adventitious defect types (17 of 25 cases). SWID, SRISE, and SLEN were the next most frequently significant variables, identified in 8, 7, and 6 of the stepwise analyses, respectively. Defect surface area was a significant predictor variable of internal features in only three cases.

Analyzing the predictor equations using the model testing samples showed that the models perform well. The correlations for halfway-in length and total depth were significant for all defect types ($p < 0.01$). The correlation coefficient R ranged from 0.37 to 0.79, and 0.45 and 0.90 for halfway-in length and depth, respectively. The correlation between halfway-in width and the predictor equations was significant for all defect types with the exception of adventitious knot clusters. For halfway-in width the correlation coefficient R ranged from 0.29 to 0.87. Correlations with clear area were significant only for medium and heavy distortions with correlation coefficients of 0.52 and 0.38, respectively. The MAE in these two cases was 15 and 20 mm for heavy and medium distortions, respectively. Although the clear area MAE for these defect types could be regarded as low, they indicate that the equations are accurate to approximate 30-mm precision (i.e.: ±15 mm). It is not clear if this level of precison is adequate for use in optimizing log-breakdown. For the distortion and adventitious defects with the model testing sample, none of the rake angle models provided a significant correlation ($p < 0.01$).

CONCLUSIONS

Overall, the strongest correlations, both model development and testing, occurred with the most severe defect types (OK, OKC, SK, UK). These are also the most recently occurring defects on the tree and have had the least time to be encapsulated or grown over. Thus, more detail about the surface indicator exists. Conversely, some of the weakest correlations that were discovered involved the least severe defect types (AK, AKC, LD, MD, HD). The adventitious knots/buds and the light and medium distortions were the oldest defects examined and had the longest time to encapsulate. Thus, less surface indicator existed for these defect types. A heavy distortion defect is at the point in the encapsulation process where an overgrown knot has made the transition to a distortion defect. More surface indicator detail exists for this type of distortion than the others. This was evident in the predictive power of the HD feature models when compared to the MD and LD defect models.

The goal of this research was to develop models capable of predicting internal defect features based on external defect characteristics. The results from this study indicate that most internal

defects can be accurately estimated using external feature data. In the future, a surface defect detection methodology developed by Thomas (2006) that uses a high-resolution laser scanner and novel detection strategies to locate severe defects on hardwood log surfaces will be coupled with the defect prediction models derived here to create a system with the speed and low cost of a laser surface scanner, but with internal defect predictive powers.

ACKNOWLEDGMENTS

The author would like to thank Al Waldron and the West Virginia Division of Forestry for donating the sample trees from the Camp Creek State Forest for this research and helping with sample collection. We also would like to thank Robert Driscole and the staff at the WVU Experimental Forest for their assistance in sample collection.

REFERENCES

CARPENTER, R. D. 1950. The identification and appraisal of log defects in southern hardwoods from surface indicators. Talk delivered at the Deep South Section—Forest Products Research Society Annual Meeting, Memphis, TN. Oct. 26, 1950. (unpublished).

——— D. L. SONDERMAN, AND E. D. RAST. 1989. Defects in hardwood timber. Ag. Handbook 678. USDA, Washington, DC. 88 p.

CHANG, S. J. 1992. External and internal defect detection to optimize the cutting of hardwood logs and lumber. Transferring technologies to the hardwood industry: Handbook No: 3. U.S. Dept. of Commerce, Beltsville, MD. ISSN 1064–3451.

HYVARINEN, M. J. 1976. Measuring quality in standing trees—Depth of knot-free wood and grain orientation under sugar maple bark distortions with underlying knots. PhD Dissertation. University of Michigan. 142 pp.

KOMSTA, L. 2006. Processing data for outliers. R News, Vol. 6/2:10–13. http://cran.r-project.org/doc/Rnews/Rnews_2006-2.pdf (May 2006).

LEMIEUX, H., M. BEAUDOIN, AND S. Y. ZHANG. 2001. Characterization and modeling of knots in black spruce (picea mariana) logs. Wood Fiber Sci. 33(3):465–475.

MARDEN, R. M. AND C. L. STAYTON. 1970. Defect indicators in sugar maple: A photographic guide. Research Paper NC-37. North Central Experiment Station, USDA Forest Service. 29 pp.

R DEVELOPMENT CORE TEAM. 2006. R: A language and environment for statistical computing. R Foundation for Statistical Computing, Vienna, Austria. ISBN 3-900051-07-0, URL http://www.R-project.org. (10 June 2006).

RAST, E. D. 1982. Photographic guide of selected external defect indicators and associated internal defects in northern red oak. Research Paper NE-511. Northeastern Forest Experiment Station, USDA Forest Service. 20 pp.

——— AND J. A. BEATON. 1985. Photographic guide of selected external defect indicators and associated internal defects in black cherry. Research Paper NE-560. Northeastern Forest Experiment Station, USDA Forest Service. 22 pp.

———, ———, AND D. L. SONDERMAN. 1988. Photographic guide of selected external defect indicators and associated internal defects in black walnut. Research Paper NE-617. Northeastern Forest Experiment Station, USDA Forest Service. 24 pp.

———, ———, AND ———. 1989. Photographic guide of selected external defect indicators and associated internal defects in white oak. Research Paper NE-628. Northeastern Forest Experiment Station, USDA Forest Service. 24 pp.

———, ———, AND ———. 1990a. Photographic guide of selected external defect indicators and associated internal defects in yellow-poplar. Research Paper NE-646. Northeastern Forest Experiment Station, USDA Forest Service. 29 pp.

———, ———, AND ———. 1990b. Photographic guide of selected external defect indicators and associated internal defects in sugar maple. Research Paper NE-647. Northeastern Forest Experiment Station, USDA Forest Service. 35 pp.

———, ———, AND ———. 1990c. Photographic guide of selected external defect indicators and associated internal defects in yellow birch. Research Paper NE-648. Northeastern Forest Experiment Station, USDA Forest Service. 25 pp.

SCHULTZ, H. 1961. Die beureilung der Qualitätsentwicklung junger Bäum, Forstarchiv, XXXII (May 15, 1961), p. 97.

SHIGO, A. L. AND E. VH. LARSON. 1969. A photo guide to the patterns of discoloration and decay in living northern hardwood trees. Research Paper NE-127. Northeastern Forest Experiment Station, USDA Forest Service. 100 pp.

STAYTON, C. L., R. M. MARDEN, R. G. BUCHMAN. 1970. Exterior defect indicators and their associated interior defect in sugar maple. For. Prod. J. Vol 20:2 (55–58).

STEELE, P. H., T. E. G. HARLESS, F. G. WAGNER, L. KUMAR, AND F. W. TAYLOR. 1994. Increased lumber value from optimum orientation of internal defects with respect to sawing pattern in hardwood logs. For. Prod. J. 44(3): 69–72.

———. 2006. PhD Dissertation. Virginia Polytechnic Institution, Blacksburg, VA. 160 pp.

TUSZYNSKI, J. 2006. caTools: Miscellaneous tools: I/O, moving window statistics. R package version 1.8. http://cran.r-project.org/src/contrib/Descriptions/caTools.html (10 October 2007)